Journal Pre-proof

A study on the initiation processes of white etching cracks (WECs) in AISI 52100 bearing steel

J. Spille, J. Wranik, S. Barteldes, J. Mayer, A. Schwedt, M. Zürcher, T. Lutz, L. Wang, W. Holweger

PII: S0043-1648(21)00253-2

DOI: https://doi.org/10.1016/j.wear.2021.203864

Reference: WEA 203864

To appear in: *Wear*

Received Date: 4 September 2020

Accepted Date: 4 March 2021

Please cite this article as: J. Spille, J. Wranik, S. Barteldes, J. Mayer, A. Schwedt, M. Zürcher, T. Lutz, L. Wang, W. Holweger, A study on the initiation processes of white etching cracks (WECs) in AISI 52100 bearing steel, *Wear*, https://doi.org/10.1016/j.wear.2021.203864.

A study on the initiation processes of white etching cracks (WECs) in AISI 52100 bearing steel

J. Spille [a,*], J. Wranik [b,e], S. Barteldes [a,c], J. Mayer [a], A. Schwedt[a], M. Zürcher [b], T. Lutz [d], L. Wang [e], W. Holweger [e,f]

[a] Central Facility for Electron Microscopy (GFE), RWTH Aachen University, Ahornstr. 55, 52074 Aachen, Germany

[b] Zeller+Gmelin GmbH & Co. KG, Schlossstraße 20, 73054 Eislingen/Fils, Germany

[c] Qass GmbH, Schöllinger Feld 28, 58300 Wetter, Germany

[d] NMI Natural and Medical Sciences Institute at the University of Tübingen, Markwiesenstr. 55, 72770 Reutlingen, Germany

[e] National Centre for Advanced Tribology at Southampton (nCATS), Mechanical Engineering Department, School of Engineering, Faculty of Engineering and Physical Sciences, University of Southampton, Southampton SO17 1BJ, United Kingdom

[f] Technology Consultant, Sailegärten 2, 72351 Erlaheim, Germany

*Corresponding author. E-mail address: spille@gfe.rwth-aachen.de

Abstract

The life cycle of any drive train is given by the reliability of its individual components, e.g., bearings, gears, and their connections. Lubrication as a part prevents wear caused by uncontrolled mixed friction. However, lubricants may interfere in the load capacity of the steel due to chemical and physical processes. White etching crack (WEC) failures are one of the most prominent failure mechanisms supposed to be related to this topic. In order to understand its initiation and progression we carried out a series of tests in the FE8 test rig proven to reproduce WEC by lubrication chemistry. These tests were stopped at an early stage.

All lubricant compositions leading to WECs showed pores in the subsurface starting in a depth of about 80 µm as an early state phenomenon, while oils not leading to WEC did not show any changes in a comparable test time. Modifications of the microstructure like new grain boundaries were found next to the pore sites by the use of SEM BSE imaging and EBSD mappings. The present investigations give valuable insight into the formation mechanisms of WECs and on the role of different lubricants in the failure process.

Keywords: White Etching Cracks (WECs), Electron Microscopy, AISI 52100, Subsurface Failure

1. Introduction

Drive trains are expected to be reliable within the life cycle. Reliability is to ensure a predictable life expectation of drive train components, e.g., gears, clutches, and bearings given by construction guidelines. Construction guidelines ensure the reliability of service life, based on the assumption that impacting load causes life reduction. For bearings the reliability is expressed by the ISO 281 standard, as the ratio of the real dynamic load rating C, the dynamic equivalent mean load P_m, and the nature of the contact p (point or line, depending on bearing type) as shown in equation (**1**) [1].

$$\boldsymbol{L_{10} = a_{ISO}(C/P_m)^p} \quad (1)$$

The real dynamic load rating C in this equation is listed as a catalogue value for bearings under standard conditions and expresses the dynamic load resulting in 10^6 revolutions, e.g., load cycles for 90 % of the bearings. The dynamic equivalent mean load P_m combines thrust and radial load impacting on the bearing. In order to reduce test time,

the dynamic loading is chosen such that a failure of the tested components is expected in a reasonable time defined as a number of load cycles passing the contact zone of a bearing. Lubrication is considered to influence the reliability in service life due to basic parameters, such as oil cleanliness, oil viscosity, and oil temperature. These parameters are summarized in a life modification factor a_{ISO}. However, plenty of studies prove that service life may depend on the composition of lubricants [2] [3].

White etching cracks (WECs) or white structure flaking (WSF) have occurred in the life cycle as a matter of maximum unreliability in bearing technology in plenty of applications [4] [5] [6] [7], but seemingly not related to any construction guideline expressed in the ISO 281. Hydrogen as a facilitator or root cause is intensely discussed worldwide [8] [9] [10] [11]. Besides, adiabatic shear bands as a result of pressure peaks were suggested to cause WEC in earlier discussions [12] [13]. Furthermore, electrical and electrostatic effects [14] [15] or combined effects with hydrogen embrittlement are known to facilitate WEC. Intense material studies on WEC features, still ongoing, prove a pronounced degradation of primary carbides, chromium depletion, and crack network formation in various depths of through hardened steels, both martensitic and bainitic, but also on case hardeners [16]. Within the past few years, tests came up to clarify the processes leading to WEC. A methodology separating the WEC features into drivers and accelerators was presented by Evans [17] such as electrical impact, water, slip and others [17] [18]. Moreover, lubricants and their components appear to be crucial for creating WEC [19] [20] [21] [22] [23] [24] [25] [26] [27] [28]. Friction energy accumulation combined with the formation of hydrogen is assumed as a possible mechanism. A recent study however points out that specific lubricants are leading to WEC, despite the fact that their friction coefficient is equal. This makes the assumption of friction energy accumulation less plausible [29].

The question how the processes leading to WEC are getting initiated remains unanswered. A recent study has proven that WEC starts in an early stage by the occurrence of subsurface cracks, emerging towards crack networks, first without white etching features, but in a later stage creating them to a high extent [30]. Within this study, WECs were provoked by the use of a low reference oil with plenty of functional additives in combination with a continuous low-level electrical impact. WECs did not occur by the use of a non-additive base oil with the same level of electrical impact. These tests show the pronounced influence of electricity in a low-level magnitude in combination with the oil chemistry, even under full film lubrication [30].

The aforementioned tests were carried out under full film lubrication ($\kappa > 3$). Other tests like FE8 show WEC under boundary lubrication ($\kappa << 1$) by the use of different oil compositions [16], but not being exposed to a low level imposed artificial electricity. A recent study is proving the pronounced influence of lubrication chemistry by the use of artificial intelligent techniques [28].

The present study aims to identify possible initiation processes of WEC failures under the given conditions of an FE8 test rig.

2. Experimental details

2.1 Rolling contact test rig

A standard FE8 test rig (Schaeffler) is used for the roller bearing tests. A sketch of the test head is shown in Figure 1. In order to keep the temperature constant a fan for the test head, a thermo-couple, and a heat exchanger for the oil were used. The temperature of the two cylindrical roller thrust bearings (CRTBs) and the lubricant was measured and recorded by the use of a thermo-couple. The test head was placed into a mounting

press and the axial load was controlled by a load cell. The CRTBs (AISI 52100 steel, martensitic hardened, 10 -12 % retained austenite, type 81212) consist of a shaft washer, a housing washer and 15 rolling elements (all AISI 52100). The rolling elements were guided by a brass cage. The axial load was set to 60 kN, resulting in a contact pressure of 1900 MPa. The rotational speed of the shaft was adjusted to 750 revolutions per minute. The maximum bearing temperature was pre-set to 100 °C, the oil flow rate on the bearings to 0.12 L/minute. The κ-value was calculated < 0.5 defining the test to be within a mixed friction regime.

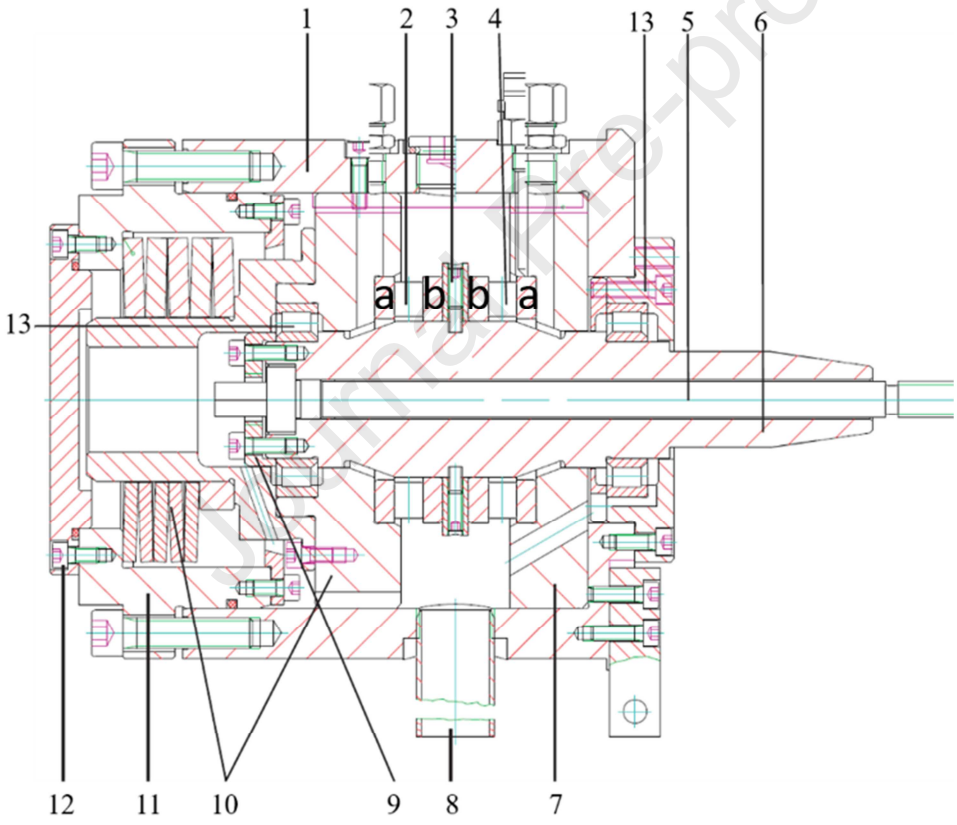

Figure 1: Test head with axial cylindrical roller bearings. 1 housing, 2 test bearing 2, 3 spacer, 4 test bearing 1, 5 shaft, 6 clamping bolt, 7 bearing seat, 8 drain pipe, 9 cap, 10 bearing support with screwed-on pilot pin, 11 lid cup of spring package, 12 lid, 13 auxiliary bearing. Both test bearings consist of a housing and a shaft washer. The two shaft washers (b) are mounted on the shaft and rotate during testing; the two housing washers (a) are embedded in the housing/support.

2.2 Chemicals

The low reference oil used in this study consists of three components, which are described as follows.

Polyalphaolefine (PAO) is registered in the EU under 500-183-1. This base oil is called high reference, not leading to WEC within the present work. Measured property data of this base oil are given in Table 1. Inductively coupled plasma optical emission spectroscopy (ICP-OES) analysis shows only traces of metallic components in the magnitude of 1-3 ppm. The low reference oil was produced by the use of this PAO as a base oil, then adding a Zinc di(2-ethylhexyl)dithiophosphate additive (ZDDP) (EC list no. 224-235-5). ICP-OES shows 8.7 wt. % zinc, 7.4 wt. % phosphorus, and 15.1 wt. % sulphur. Moreover, a dicyclohexylamine additive (DCHA) (EU 202-980-7) was added. The composition of the low reference oil is shown in Table 2. The purity is guaranteed to be >99 % with a water content < 0.3 %.

In order to carry out the test runs on the FE8 test rig, 7 kg of the lubricant were produced by mixing the components at 40 °C until reaching a clear solution. Measured data of this low reference oil is listed in Table 1. As dicyclohexylamine shows a certain deliquescence, the lubricant was produced immediately prior to the tests or stored under nitrogen atmosphere.

Table 1: Lubricant parameters of the low and high reference oil used in this study

Parameter	**Standard**	**Low Reference Oil**	**High Reference Oil (PAO)**
Optical assessment		no color, clear,	No color, clear, no

		no sludge	sludge
Color	DIN ISO 2049	L0.5	L 0.5
viscosity 40 °C [mm²/s]	ASTM D 7042	44.3	46.3
viscosity 100 °C [mm²/s]	ASTM D 7042	7.4785	7.85
viscosity index [-]	ASTM D 2270	135	140
density 15 °C [g/cm³]	DIN EN ISO 12185	0.839	0.832
refractive index [-]	DIN 51423-2	1.4635	1.4621
water content (procedure C) [%]	E DIN 51777	<0.01	<0.01
TAN [mg KOH/g]	DIN EN 12634	2.9	<0.1
Sulphur [ppm] mean value		3832	
Sulphur [ppm] standard deviation of the mean		24	
Phosphorus [ppm] mean value		1840	
Phosphorus [ppm] standard deviation of the mean		24	
Zinc [ppm] mean value		2133	
Zinc [ppm] standard deviation of the mean		42	

Table 2: Overview of the conducted tests and lubricant composition

Test runs

Test number	Lubricant description	Lubricant composition	FE8 runtime	Result Washer	Result Rolling Elements
1	High ref	100 % PAO	18h	No spalling	No spall-ing
2	Low ref	95 % PAO 2.5 % DCHA 2.5% ZDDP	72 h	Spalling	Spalling
3	Low ref	95 % PAO 2.5 % DCHA 2.5% ZDDP	15 h	No spalling	No Spalling

2.3 Materials investigation

All investigations were carried out using the washers of the bearings (Figure 1, test rig) divided into a housing washer and a shaft washer. Investigations on rollers are part of further investigations.

The preparation is summarized schematically in Figure 2 a. The samples were visually inspected first, documenting the alterations using a stereomicroscope (Figure 2 b). After inspection, the samples were cut and afterwards prepared by mechanical grinding on silicon carbide papers up to grits of about 10 µm average grain size and polishing with 6, 3, 1, and 0.25 µm diamond suspensions for at least 5 minutes (Figure 2). The prepara-

tion was finished by the usage of a 50 nm colloidal silica suspension. After nital-etching, the samples were re-polished. Panorama images were carried out to search a comparatively large area for possible modifications of the microstructure. Three panorama images were executed from test no. 3. They were taken from (I) directly below the surface alterations, (II) in the same depth than the first one but not below the surface alterations, and (III) in a depth of approximately 1.5 mm below the raceway surface as can be seen in Figure 2 a. The extension of such a panorama region is visible by the contamination after collection (Figure 2 c). Furthermore, one panorama was executed from the samples of test no. 1 and 2 each. All panoramas are shown in the supplementary material.

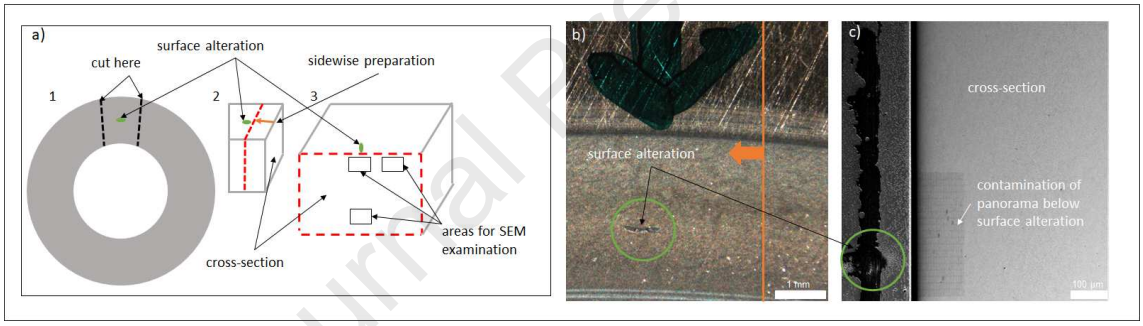

Figure 2: a) Schematic summary of the preparation. b) Stereomicroscope image of a surface alteration (green circle) from the bearing of test no. 3. The orange arrow indicates the direction of preparation. c) SEM image showing part of the surface alteration (green circle) as well as the contamination of a panorama below the alteration. The sample was tilted by 60° and the contrast was adjusted while the image acquisition to show both, the surface alteration as well as the prepared surface. Note that a grey-value correction was applied to show the contamination more clearly.

Scanning electron microscopy-electron backscatter diffraction (SEM-EBSD) measurements were carried out using a JEOL JSM7000F field emission gun SEM equipped with the combined EDS/EBSD system Pegasus by Ametek-EDAX. EBSD measurements were performed at an acceleration voltage of 15 kV and a working distance of 15 mm. Data evaluation of EBSD measurements was performed using OIM Analysis version 8.

The maps shown in this work are quite comparable to previous work done by Rumpf [31] [32] and by Diederichs [33]. However, for a better understanding, the different maps are briefly described below. For recording secondary electron/backscattered electron (SE/BSE) images, a Zeiss GeminiSEM 300 field emission gun SEM was used. Images were taken at an acceleration voltage of 10 kV and a working distance of 5 - 7 mm if not stated otherwise. Automated panoramas were collected in order to search large areas at high magnification for alterations in the microstructure. The panorama software SmartStitch (Zeiss), which is an add-on of the SmartSEM software, was used. Due to their sizes, only sections are shown here but representing the overall picture (cf. the supplementary material of the web version of this article for the complete, high-resolution panoramas).

Image quality (IQ) maps based on EBSD data are used for the visualization of the microstructure. The IQ maps visualize the quality of the diffraction patterns at each individual pixel. The contrast in these maps originates from several sources like phases, strain, topography, and defects in the crystal structure [34] as well as from the orientation.

Kernel average misorientation (KAM) maps show the average misorientation between a point and selected neighbors (e.g., all neighbors in 100 nm distance) in the same grain. KAM maps are used to visualize local lattice deformation, e.g., due to dislocations [35].

Within a phase map, each point is colored according to the assigned “phase”. Since the differences between lattice parameter a and c are too small to detect the tetragonality of martensite, the body-centered cubic (bcc) α-Fe was chosen for indexing [36]. Further distinction between the individual body-centered components in steels is only possible based on secondary parameters like IQ or KAM. Other phases chosen for indexing pur-

poses are face-centered cubic (fcc) γ-Fe representing austenite and cementite representing $(Fe,Cr)_3C$.

Non martensite-martensite (NonMs-Ms) maps show those high-angle grain boundaries, which cannot be explained by a martensitic phase transformation. In an undistorted martensitic microstructure, these usually are given by prior austenite grains. However, they also show newly formed grain boundaries, which may have formed during strain or recrystallization. For NonMs-Ms maps, a neighbor confidence index (CI) correlation clean up with CI>0.1 was applied to the data.

3. **Results and discussion**

3.1 Run until failure

The first test was performed until surface failure occurred, showing that the chosen testing parameters together with a low reference oil are able to produce WEAs after sufficiently long runtimes in repetition. The experiment stopped automatically after about 72 h due to large spalling on the raceway surface (Figure 3 a).

3.1.1 Surface characterization

A large spalled area is visible on the raceway surface of the washer. A metallographic cross-section close to the edge of the spalling was prepared perpendicular to the rolling direction (Figure 3 a).

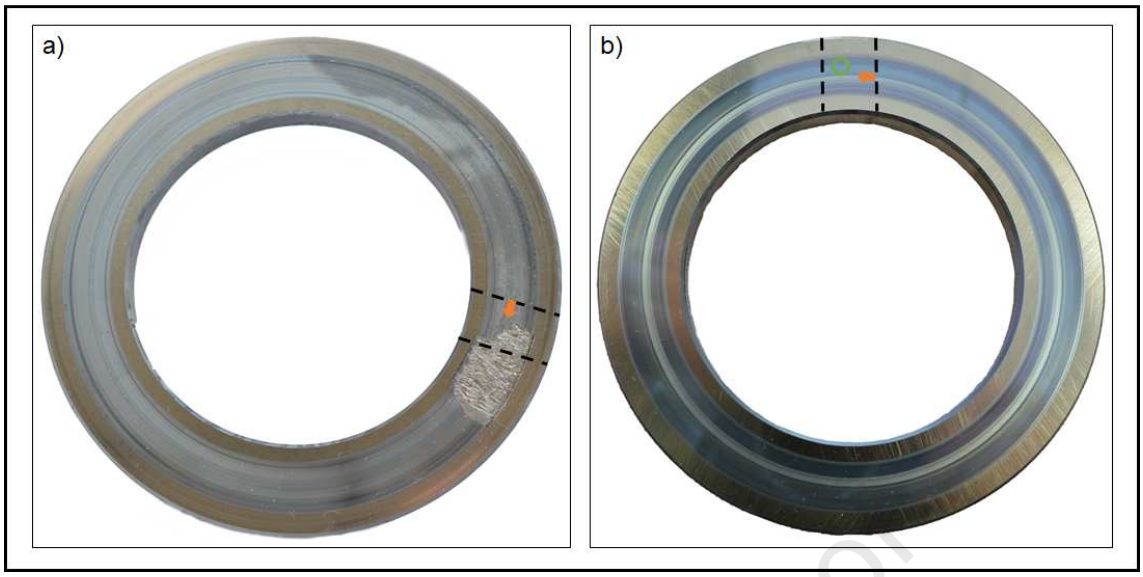

Figure 3: Sample sites of two bearings chosen for this work. a) Bearing corresponding to test no. 2 b) Bearing corresponding to test no. 3. The black, dashed lines show the areas where the samples were cut and the orange arrows indicate the direction of preparation. The location of the alteration on the raceway of the bearing from test no. 3 is shown by the green circle. This alteration was already shown in Figure 2 b and c.

3.1.2 Subsurface characterization

A crack with a length of about 200 µm was found in the subsurface, at a depth of approximately 100 µm, using light optical microscopy (LOM) (Figure 4). Nital etching points out that this crack is accompanied by a small WEA (see arrows within Figure 4). SEM BSE panoramas/images were taken and an EBSD measurement was performed in a re-polished state to analyze the character of the microstructure alterations (Figure 4 b-f). The BSE panorama clearly shows a crack together with a nano-crystalline region surrounding it, whereas the rest of the matrix seems to be unaffected and shows a typical AISI 52100 microstructure consisting of martensite and spherical $(Fe,Cr)_3C$ carbides. The WEA is located mainly on one side of the crack (Figure 4 b, arrow). The EBSD phase map shows that the matrix consists of phases indexed as bcc and carbides whereas retained austenite is not present (Figure 4 c). Inside the WEA there are a few

ferrite grains showing a high image quality as well as low KAM values indicating that they are rather composed of ferrite than martensite. However, the main part of the WEA is too fine-crystalline for EBSD analysis and consequently shown in black since it could not be indexed. The KAM values next to the crack seem to be slightly elevated (Figure 4 d, e). Furthermore, the NonMs-Ms map reveals that the grains inside the WEA are newly formed (Figure 4 f), which is in good agreement with the high IQ and low KAM values.

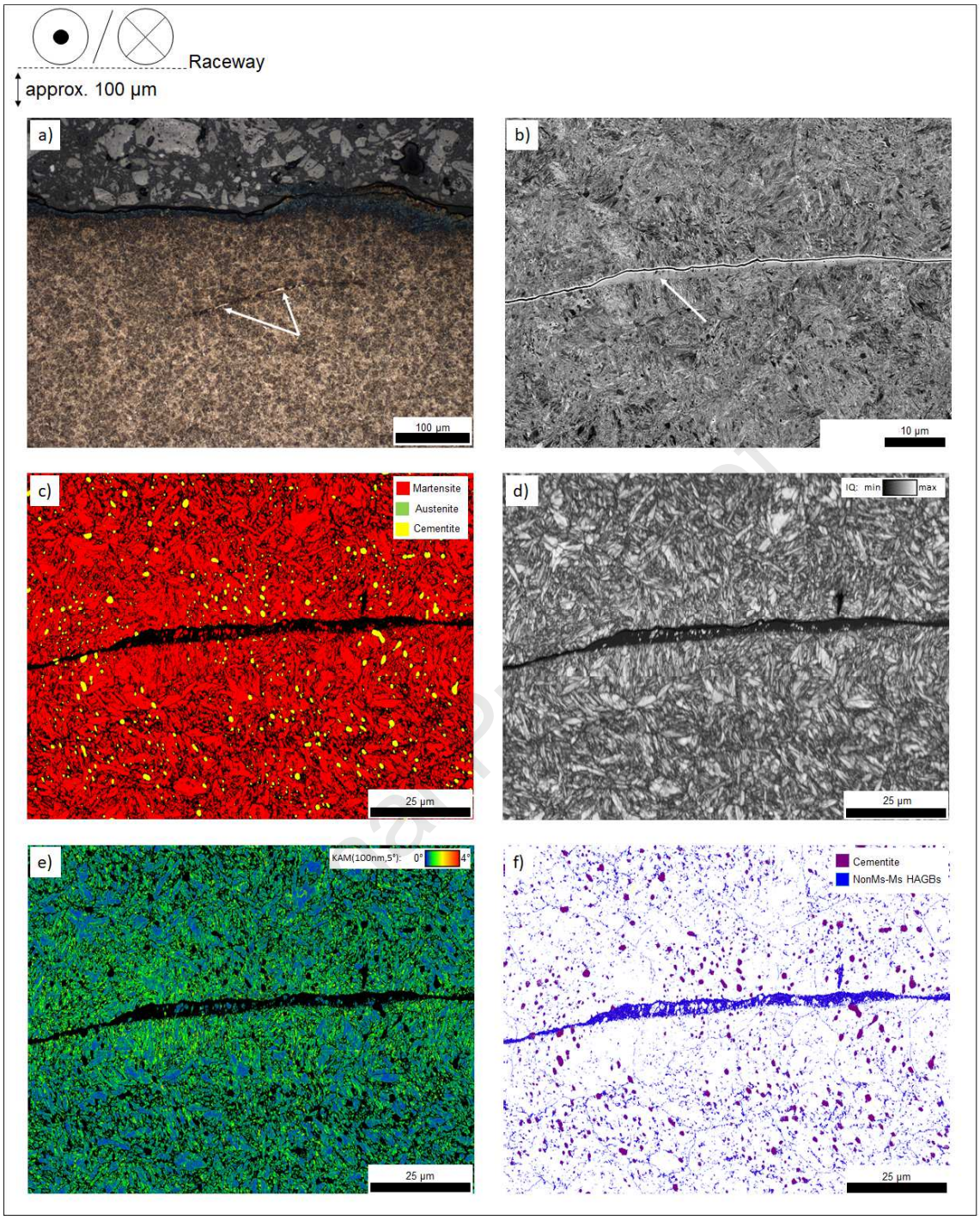

Figure 4: LOM, BSE and EBSD images taken for a subsurface characterization of the sample from the bearing corresponding to test no. 2. a) LOM image in a nital-etched state showing a crack together with WEA. b) BSE panorama of the WEA in a re-polished state approximately 100 µm below the raceway surface. Note that a grey-value correction was applied to the BSE panorama to show the WEA more clearly. c) EBSD phase map. Black dots within the phase map are points, which were excluded due to the confidence index criterion (CI<0.1). d) EBSD IQ map. e) EBSD KAM map of martensite based on the second neighbor. The step size is 50 nm. Black dots within the phase map are points, which were exclud-

ed due to the confidence index criterion (CI<0.1). f) NonMs-Ms map of the WEA. Note that a neighbor CI correlation clean up with CI>0.1 was applied to the data. The pictures b-f only show a small section of the whole WEA.

Figure 4 clearly shows that the chosen testing parameters are able produce WEAs after sufficiently long runtimes. Hence, possible microstructural alterations from stopped tests can be seen as possible precursors to WEA formation.

3.2 Interrupted tests

In order to identify earlier stages of WEA formation, tests with a low reference oil were stopped after 15 hours. Additionally, tests with high reference oils were carried out for comparison.

3.2.1 Surface characterization of the low reference oil

For the low reference oil visible alterations on the raceway surface (note the feature about 800 µm in length in Figure 2 b) are identified by stereomicroscopy. A segment around the altered surface was prepared perpendicular to the rolling direction as shown for the bearing of test no. 3 (Figure 3 b).

3.2.2 Subsurface characterization of the low reference oil

The subsurface underneath the surface alterations was characterized by SEM panorama images (SE and BSE) and EBSD measurements. Plenty of pores were found below the surface alterations however, not in those subsurface segments where the surface was unaffected. Some interesting areas of higher magnification are shown in Figure 5 and the upper half of Figure 6. Pores were found neither within the high reference samples

(test run with the pure base oil (PAO)) nor in a sample of the original material, respectively.

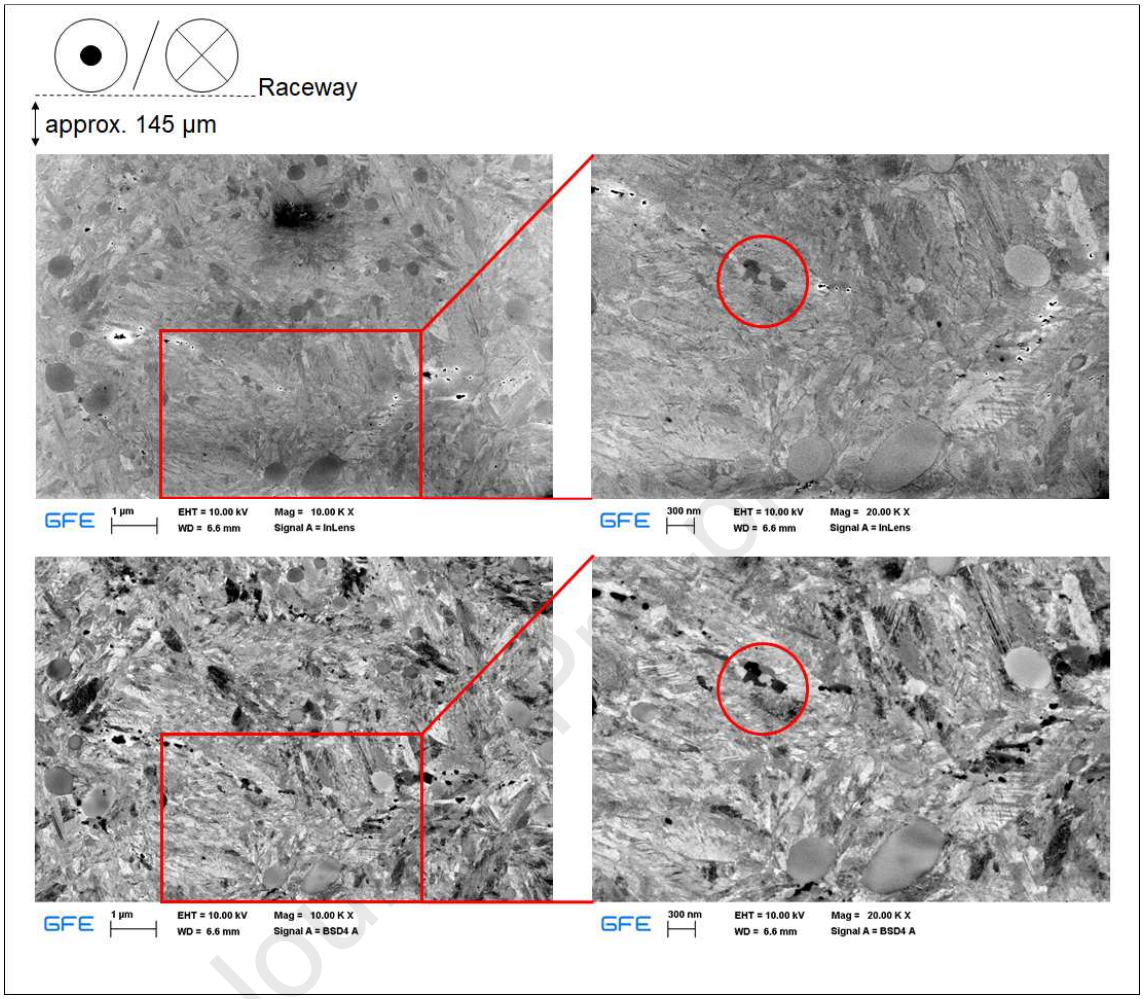

Figure 5: SE and BSE images of pores in the sample from the bearing corresponding to test no. 3 in a depth of approximately 145 µm below the surface alteration. Note that a grey-value correction was applied to the images to show the pores more clearly. Slight alterations of the microstructure with some possible newly formed grains can already be observed in the vicinity of the pores (red circle). The dark area in the left SE image results from contamination due to focusing.

Obviously, the microstructure has changed in some regions next to the pores. These changes in the microstructure look like being newly formed grains, in accordance to the ones seen in fully developed WEAs as well. The NonMs-Ms maps sometimes also show the existence of newly formed grains. These grains are also visible in the corresponding

IQ map (Figure 6). A comparison of SE and BSE images with an EBSD measurement is shown in Figure 6.

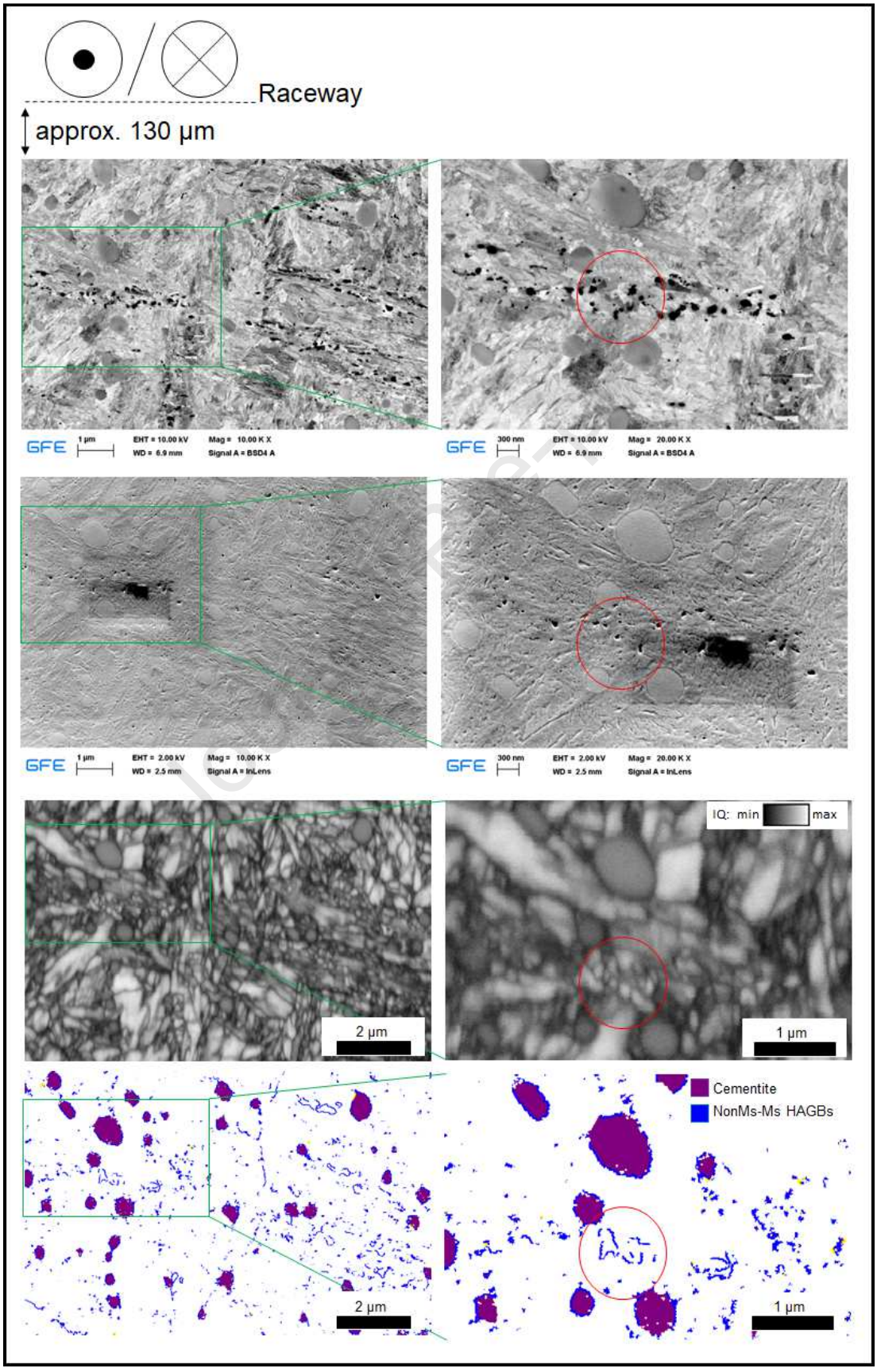

Figure 6: Correlation of SE and BSE images with an IQ and a NonMs-Ms map derived from an EBSD measurement on the sample from the bearing corresponding to test no. 3. The area of interest is approximately 130 µm below the surface alteration. It can be seen that there are some newly formed grains within the red circle. Note that a neighbor CI correlation clean up with CI>0.1 was applied to the data for the NonMs-Ms map. The step size of the EBSD measurement was 25 nm. Note that the in-lens images were acquired at 2 kV and a working distance of 2.5 mm to show the pores more clearly. A grey-value correction was applied to the SEM images to show the pores more clearly. The dark area in the SE images results from contamination due to focusing.

A comparison of SE and BSE images with the corresponding EBSD measurement shows that there are newly formed grains in the vicinity of the pores. The pores in the subsurface give a hint that this area was subjected to high localized energy impact. As a matter of the high degree of localized energy, it is also possible that WEA and WEC are a later consequence.

4. Conclusions

The results are showing that the processes leading to WEC formation caused by the use of a low reference oil show the formation of pores in an early stage. All those tests lead to WEC in progression. None of these processes were observed in the case of a high reference oil test run. We assume that the formation of the pores is due to the effect of surface alterations caused by the chemicals used in the low reference tests. The relation between those chemicals, the visible surface alterations, and the latter formation of WEC has to be studied in more detail. We conclude that the pores, accompanied by a change in the microstructure, facilitate the formation of WEC in a later stage due to the fact that the loading and subsequent degradation gets increasingly localized. Localization of the loading in combination with a weakening of the material around the pores

might be the cause of the formation of white etching areas and the subsequent initiation of cracks and crack networks.

5. Acknowledgements

The authors would like to thank Zeller+Gmelin GmbH&Co. KG and Qass GmbH for the support in this study. JS and JM acknowledge the support of the DFG in the frame-work of project MA 1280/57-1.

References

[1] *Rolling bearings - Dynamic load ratings and ratings life,* BS ISO 281, BSI, Mar 2007 (incorporating corrigendum May 2008).

[2] M. A. Chowdhury (Ed.), Friction, Lubrication and Wear, IntechOpen, 2019.

[3] M. Reichelt, T. E. Weirich, J. Mayer, T. Wolf, J. Loos, P. W. Gold and M. Fajfrowski, "TEM and nanomechanical studies on tribological surface modifications formed on roller bearings under controlled lubrication conditions," *Journal of Materials Science,* vol. 41, no. 14, p. 4543–4553, 2006.

[4] K. Tamada and H. Tanaka, "Occurrence of brittle flaking on bearings used for automotive electrical instruments and auxiliary devices," *Wear,* vol. 199, no. 2, pp. 245-252, 1996.

[5] N. Kino and O. Keizo, "The influence of hydrogen on rolling contact fatigue life and its improvement," *JSAE review*, vol. 24, no. 3, pp. 289-294, 2003.

[6] H. Harada, T. Mikami, M. Shibata, D. Sokai, A. Yamamoto and H. Tsubakino, "Microstructural changes and crack initiation with white etching area formation under rolling/sliding contact in bearing steel," *ISIJ international,* vol. 45, no. 12, pp. 1897-1902, 2005.

[7] J. Gegner, "Tribological Aspects of Rolling Bearing Failures," *InTech Europe,* pp. 33-94, 2011.

[8] A. Ruellan, Tribological analysis of White Etching Crack (WEC) failures in rolling element bearings. Mechanics of materials [physics.class-ph], INSA de Lyon (PhD-Thesis), 2014.

[9] H. K. D. H. Bhadeshia and W. Solano-Alvarez, "Critical assessment 13: elimination of white etching matter in bearing steels," *Materials Science and Technology*, vol. 31, no. 9, pp. 1011-1015, 2015.

[10] K. Stadler, J. Lai and R. Vegter, "A review: the dilemma with premature white etching crack (WEC) bearing failures," *Bearing Steel Technologies: 10th Volume, Advances in Steel Technologies for Rolling Bearings. ASTM International,* pp. 487-508, 2014.

[11] M. Kohara, T. Kawamura and M. Egami, "Study on mechanism of hydrogen generation from lubricants," *Tribology Transactions,* vol. 49, no. 1, pp. 53-60, 2006.

[12] W. Solano-Alvarez, J. Duff, M. C. Smith and H. K. D. H. Bhadeshia, "Elucidating white-etching matter through high-strain rate tensile testing," *Materials*

Science and Technology, vol. 33, no. 3, pp. 307-310, 2017.

[13] S. W. Ooi, A. Gola, R. H. Vegter, P. Yan and K. Stadler, "Evolution of white-etching cracks and associated microstructural alterations during bearing tests," *Materaisl Science and Technology,* vol. 33, no. 14, pp. 1657-1666, 2017.

[14] J. Loos and I. Bergmann, "Influence of Currents from Electrostatic Charges on WEC Formation in Rolling Bearings," *Tribology Transactions,* vol. 59, no. 5, pp. 865-875, 2016.

[15] M. Ščepanskis, B. Gould and A. Greco, "Empirical Investigation of Electricity Self-Generation in a Lubricated Sliding–Rolling Contact," *Tribology Letters,* vol. 65, no. 3, p. 109, 2017.

[16] W. Holweger, M. Wolf, D. Merk, T. Blass, M. Goss, J. Loos, S. Barteldes and A. Jakovics, "White etching crack root cause investigations," *Tribology Transactions,* vol. 58, no. 1, pp. 59-69, 2015.

[17] M. H. Evans, "An updated review: white etching cracks (WECs) and axial cracks in wind turbine gearbox bearings," *Materials Science and Technology,* vol. 32, no. 11, pp. 1133-1169, 2016.

[18] J. Lai and K. Stadler, "Investigation on the mechanisms of white etching crack (WEC) formation in rolling contact fatigue and identification of a root cause for bearing premature failure," *Wear,* Vols. 364-365, pp. 244-256, 2016.

[19] H. Danielsen, F. Gutiérrez Guzmán, K. Dahl, Y. Li, J. Wu, G. Jacobs, G. Burghardt, S. Fæster, H. Alimadadi, S. Goto, D. Raabe and R. Petrov, "Multiscale characterization of White Etching Cracks (WEC) in a 100Cr6 bearing from a thrust bearing test rig," *Wear,* vol. 370, pp. 73-82, 2017.

[20] A. M. Diederichs, S. Barteldes, A. Schwedt, J. Mayer and W. Holweger, "Study of subsurface initiation mechanism for white etching crack formation," *Materials Science and Technology,* vol. 32, no. 11, pp. 1170-1178, 2016.

[21] J. Franke, J. Carey, S. Korres, T. Haque, P. Jacobs, J. Loos and W. Kruhoeffer, "White etching cracking—simulation in bearing rig and bench tests," *Tribology Transactions,* vol. 61, no. 3, pp. 403-413, 2017.

[22] B. Gould, N. G. Demas, G. Pollard, J. J. Rydel, M. Ingram and A. C. Greco, "The effect of lubricant composition on white etching crack failures," *Tribology Letters,* vol. 67, no. 1, 2019.

[23] F. G. Guzmán, M. Oezel, G. Jacobs, G. Burghardt, C. Broeckmann and T. Janitzky, "Reproduction of white etching cracks under rolling contact loading on

thrust bearing and two-disc test rigs," *Wear,* vol. 390, pp. 23-32, 2017.

[24] T. Haque, S. Korres, J. T. Carey, P. W. Jacobs, J. Loos and J. Franke, "Lubricant effects on white etching cracking failures in thrust bearing rig tests," *Tribology Transactions,* vol. 61, no. 6, pp. 979-990, 2018.

[25] M. Paladugu, D. R. Lucas and R. S. Hyde, "Effect of lubricants on bearing damage in rolling-sliding conditions: Evolution of white etching cracks," *Wear,* vol. 398, pp. 165-177, 2018.

[26] F. Pape, J. Terwey, S. Wiesker, S. Averbeck, C. Muhmann, D. Lipinsky, H. Arlinghaus, E. Kerscher, B. Sauer and G. Poll, "Tribological research on the development of White Etching Cracks (WECs)," *Forschung im Ingenieurwesen,* vol. 82, no. 4, pp. 341-352, 2018.

[27] A. Richardson, M. Evans, L. Wang, M. Ingram, Z. Rwoland, G. Llanos and R. Wood, "The effect of over-based calcium sulfonate detergent additives on white etching crack (WEC) formation in rolling contact fatigue tested 100Cr6 steel," *Tribology International,* vol. 133, pp. 246-262, 2019.

[28] B. Azzam, F. Harzendorf, R. Schelenz, W. Holweger and G. Jacobs, "Pattern Discovery in White Etching Crack Experimental Data Using Machine Learning Techniques," *Applied Sciences,* vol. 9, no. 24, p. 5502, 2019.

[29] A. Ruellan, K. Stadler, J. Jelita Rydel and H. Ryan, "The influence of lubricant formulation on early thrust radial bearing damage associated with white etching cracks," *Proceedings of the Institution of Mechanical Engineers, Part J: Journal of Engineering Tribology,* pp. 1-13, 2020.

[30] V. Rumpf, A Study on Microstructural Alterations in White Etching Cracks, Dark Etching Region, and White Etching Bands in Rolling Contacts, Southampton: University of Southampton (PhD-Thesis), 2018.

[31] V. Šmeļova, A. Schwedt, L. Wang, W. Holweger and J. Mayer, "Microstructural changes in White Etching Cracks (WECs) and their relationship with those in Dark Etching Region (DER) and White Etching Bands (WEBs) due to Rolling Contact Fatigue (RCF)," *International Journal of Fatigue,* vol. 100, pp. 148-158, 2017.

[32] V. Šmeļova, A. Schwedt, L. Wang, W. Holweger and J. Mayer, "Electron microscopy investigations of microstructural alterations due to classical Rolling Contact Fatigue (RCF) in martensitic AISI 52100 bearing steel," *International Journal of Fatigue,* vol. 98, pp. 142-154, 2017.

[33] A. M. Diederichs, A. Schwedt, J. Mayer and T. Dreifert, "Electron microscopy analysis of structural changes within white etching areas," *Material Science*

and Technology, vol. 32, no. 16, pp. 1683-1693, 2016.

[34] S. I. Wright and M. M. Nowell, "EBSD Image Quality Mapping," *Microsc. Microanal.*, vol. 12, no. 1, pp. 72-84, 2006.

[35] A. J. Schwartz, M. Kumar, B. L. Adams and D. P. Field, Electron Backscatter Diffraction in Materials Science, Springer Science+Buisness Media, 2009.

[36] L. Ryde, "Application of EBSD to analysis of microstructures in commercial steels," *Materials Science and Technology*, vol. 22, no. 11, pp. 1297-1306, 2006.

Highlights:

1. Early state initiation of white etching crack (WEC) formation
2. Changes of lubrication chemistry lead to a microstructure deterioration due to pores
3. Evidence of newly formed grains near the pores
4. Pores indicate areas of high localized energy impact

Declaration of interests

☒ The authors declare that they have no known competing financial interests or personal relationships that could have appeared to influence the work reported in this paper.

☐The authors declare the following financial interests/personal relationships which may be considered as potential competing interests: